EPJ Web of Conferences **364**, 01021 (2026) https://doi.org/10.1051/epjconf/202636401021
Quark Matter 2025

Experiment overview of physics of ultraperipheral collisions

Agnieszka Ogrodnik[1,2,*,**]

[1]Institute of Nuclear Physics Polish Academy of Sciences
ul. Radzikowskiego 152, 31-342 Kraków, Poland
[2]Institute of Nuclear Physics, Faculty of Mathematics and Physics, Charles University
Ke Karlovu 2027/3, 121 16 Prague, Czech Republic

Abstract. In this proceeding a summary of a selection of experimental results on ultraperipheral collisions from the XXXI International Conference on Ultra-relativistic Nucleus-Nucleus Collisions, Quark Matter 2025 is presented.

1 Introduction

Heavy ions accelerated to ultra-relativistic velocities are intense sources of electromagnetic (EM) fields, which can be interpreted as fluxes of photons. At the Relativistic Heavy Ion Collider (RHIC), these photons can reach energies of up to 3 GeV, and at the Large Hadron Collider (LHC), they can reach up to 80 GeV. In ultraperipheral collisions (UPCs), where the impact parameter b is larger than the sum of the nuclear radii, hadronic interactions are suppressed and photon-induced interactions dominate.

Two major types of interactions in UPCs can be distinguished. The first involves photon–photon interactions, which have been extensively studied for precision tests of the Standard Model and searches for Beyond Standard Model phenomena. Recent developments in photon–photon processes are summarized in Sec. 2. The second class includes photonuclear interactions, where the photon interacts directly with the nucleus, or where a photon fluctuates into a quark–antiquark pair that then interacts with the nucleus. Photonuclear processes can be further divided into coherent ones, in which photons interact coherently with the whole nucleus, and incoherent ones, in which photons interact with the nuclear substructure. A summary of recent photonuclear measurements is provided in Sec. 3, followed by the conclusions in Sec. 4.

2 Photon-photon interactions

Dilepton production has been measured by several collaborations using e^+e^-, $\mu^+\mu^-$, and $\tau^+\tau^-$ final states; see Refs. [1–9]. New differential cross-section results for $\gamma\gamma \to \tau^+\tau^-$ production

*e-mail: agnieszka.ogrodnik@cern.ch
**This work was supported by National Science Centre, Poland grant 2023/51/B/ST2/02507, by PL-Grid Infrastructure, by The Ministry of Education, Youth and Sports of the Czech Republic under project ERC-CZ LL2327 and by Charles University grant UNCE 24/SCI/016.

were recently reported by ATLAS [10], while the CMS Collaboration reported updated constraints on the τ-lepton anomalous magnetic moment [11]. Both measurements show good agreement with model predictions within experimental uncertainties.

As an extension of the $\mu^+\mu^-$ measurement, the ATLAS Collaboration recently presented a study of coincident ρ-meson and $\mu^+\mu^-$ production using Pb+Pb collision data [12]. Events were tagged via the $\gamma\gamma \to \mu^+\mu^-$ process, and the rate of ρ-meson production from the same lead–lead interaction was measured relative to the rate of exclusive $\gamma\gamma \to \mu^+\mu^-$ events. The ratio was measured as a function of dimuon mass ($m_{\mu\mu}$), dimuon rapidity ($y_{\mu\mu}$), the leading-photon energy (E_γ^{lead}), and the activity in the Zero-Degree Calorimeter (ZDC), as shown in Fig. 1. The observed trends provide new insight into the impact-parameter dependence of photon-induced vector-meson production. This measurement confirms the presence of multiphoton-induced processes in UPC collisions, emphasizing the importance of accurately evaluating exclusivity criteria.

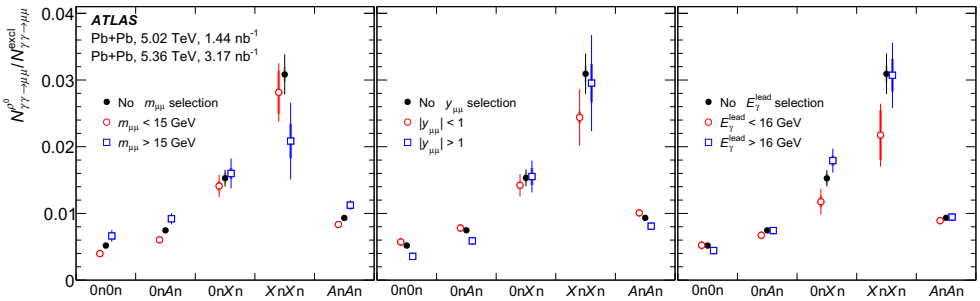

Figure 1. The ratio of coincident ρ^0 production in $\gamma\gamma \to \mu^+\mu^-$ events to the number of exclusive $\gamma\gamma \to \mu^+\mu^-$ events for different ZDC selections. The left, centre, and right panels compare different $m_{\mu\mu}$, $y_{\mu\mu}$, and E_γ^{lead} intervals, respectively. The error bars and bands indicate statistical and systematic uncertainties. The coincidence rates are measured in the fiducial acceptance of the ATLAS detector, namely $|\eta| < 2.5$ and $p_T > 100$ MeV for pions from the ρ^0 decay.

A novel example of a UPC measurement is the search for magnetic monopoles using the ATLAS UPC dataset [13]. These hypothetical particles would bend differently in a magnetic field, producing parabolic trajectories in the ATLAS tracking detectors. The number of events in the signal region was found to be consistent with background predictions, and new, more stringent constraints on the magnetic-monopole production cross-section were derived.

3 Photonuclear interactions

Photonuclear collisions provide a clean environment to study nuclear structure. Coherent particle production allows probing nuclear gluon densities, while incoherent production enables the study of fluctuations in these densities.

Observation of ϕ-meson production was reported by LHCb [14] and CMS [15]. Measurements of this process enable studies of the nuclear gluonic structure in the non-perturbative, low-Q^2 region. The left panel of Fig. 2 shows the K^+K^- mass distribution measured by LHCb, well described by a fit including contributions from ϕ mesons, misidentified ρ mesons, and dissociative and non-resonant processes. A comparison of the cross-section with various models by CMS, shown in the right panel of Fig. 2, indicates a better description of the data by shadowing models than by saturation models.

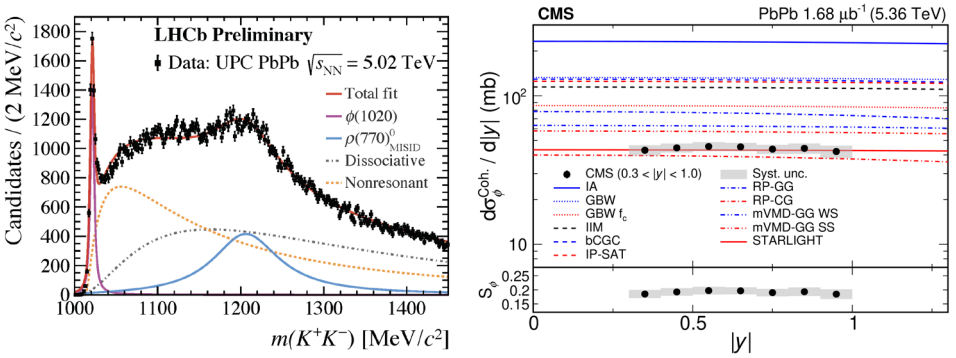

Figure 2. Left: Mass spectrum of the K^+K^- pair with a fit distinguishing contributions from the ϕ meson, misidentified ρ meson, and dissociative and non-resonant contributions measured by LHCb [14]. Right: Cross-section of coherent ϕ-meson production as a function of $|y|$ measured by CMS [15].

Higher-mass vector mesons were also studied: coherent J/ψ production was measured by STAR [16], ALICE [17, 18], CMS [19], LHCb [20], and ATLAS [21]; incoherent J/ψ production was measured by ALICE [22] and CMS [23]; and coherent Υ production was recently measured by CMS [24].

Coherent J/ψ production was measured by STAR in Ru+Ru, Zr+Zr, and Au+Au collisions at $\sqrt{s_{NN}}$ = 200 GeV. The resulting cross-sections were lower than the STARlight predictions. Additionally, a spin-interference effect, previously confirmed for ρ mesons [25], was also observed for J/ψ by STAR. The left panel of Fig. 3 shows the strength of the $\cos 2\phi$ modulation as a function of the p_T of $J/\psi \to e^+e^-$ candidates. An increasing trend from negative to positive values with rising p_T is observed. A QED model (EPA) including radiative decays and bremsstrahlung but excluding interference effects describes the increasing trend for $p_T > 0.06$ GeV, but deviates from the data at lower p_T by 2.4σ.

The most recent coherent J/ψ measurement at $\sqrt{s_{NN}}$ = 5.36 TeV was reported by ATLAS [21], providing the first LHC measurement at intermediate rapidities. After extrapolating the measured cross-sections to $\sqrt{s_{NN}}$ = 5.02 TeV, the new results agree with previous measurements from CMS and LHCb, and with the ALICE results at forward rapidities, as shown in the right panel of Fig. 3. However, the tension with the ALICE midrapidity measurement remains unexplained.

Studies of incoherent J/ψ production provide access to gluon-density fluctuations. The recent ALICE measurement of the $|t|$ dependence of the incoherent cross-section [26] shows better agreement with models including fluctuations than with those without them. The dependence of the incoherent J/ψ production on the photon–nucleus centre-of-mass energy ($W_{\gamma A}$), reported by CMS [23] and ALICE [22], also helps differentiate between theoretical models. In both analyses, events with forward-rapidity J/ψ mesons are divided into two categories according to the photon energy. As shown in the left panel of Fig. 4, the data exhibit stronger suppression at high $W_{\gamma A}$ than all model predictions, with no model describing the full measured energy range. The ALICE measurement, additionally split into three $|t|$ bins (right panel of Fig. 5), shows larger suppression at higher $|t|$, consistent with shadowing and saturation models, although saturation models provide a better overall description.

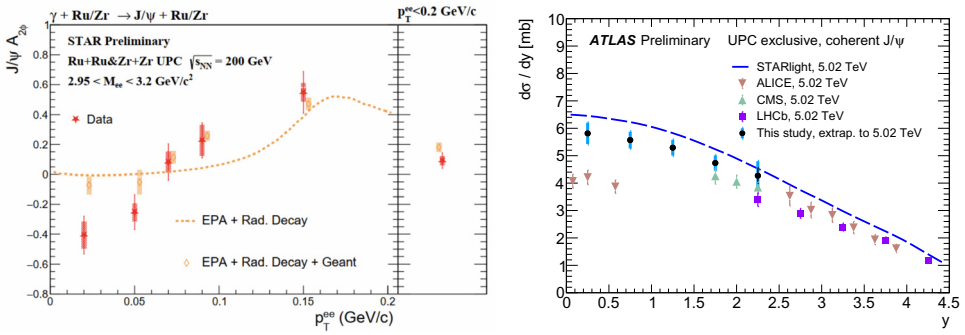

Figure 3. Left: Measurement of the modulation strength of the J/ψ meson by STAR as a function of the p_T of $J/\psi \to e^+e^-$ candidates. The result is compared with a QED model including radiative decays and bremsstrahlung but excluding interference effects. Right: Measured differential cross-section for coherent J/ψ production in Pb+Pb UPC at 5.02 TeV as a function of J/ψ rapidity. Results from ALICE [17, 18], CMS [19], and LHCb [20] are also shown, together with the ATLAS result extrapolated to 5.02 TeV. Data points are compared with STARlight predictions [21].

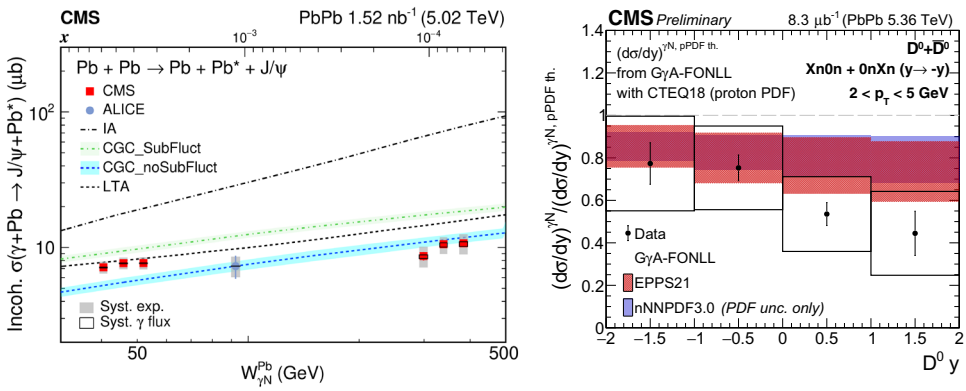

Figure 4. Left: Incoherent J/ψ photoproduction cross-section per γPb interaction as a function of $W_{\gamma N}$ (lower axis) or x (upper axis) from the CMS measurement [23], compared with IA, LTA, and CGC model predictions. Right: Ratio of D^0 production cross-sections relative to FONLL predictions using the CTEQ18 proton PDF parametrization, serving as the baseline without nuclear effects. Data (black) are compared with FONLL predictions using EPPS21 (red) and nNNPDF3.0 (purple) nuclear PDFs; only nuclear-PDF uncertainties are shown.

Open heavy flavour is a new and complementary probe in UPCs, offering broad coverage in Q^2 and x. New CMS results on the D^0 differential cross-section show hints of stronger suppression at low p_{T} and high y [27], while for D^0 mesons with $p_{\mathrm{T}} > 5$ GeV, good agreement with predictions is observed across the rapidity range [28]. The rapidity dependence of the cross-section for the lowest p_{T} bin (2–5 GeV) is shown in Fig. 4. The ALICE Collaboration reported preliminary D^0 p_{T} spectra down to $p_{\mathrm{T}} = 0$ GeV, showing that current predictions fail to describe the full p_{T} range.

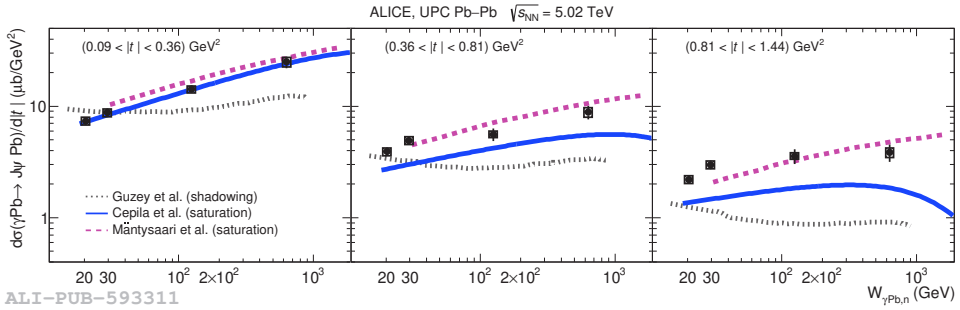

Figure 5. Energy dependence of the incoherent J/ψ cross-section from ALICE in three $|t|$ ranges, compared with shadowing-based (dot-dashed) and saturation-based (dashed and solid) models [22].

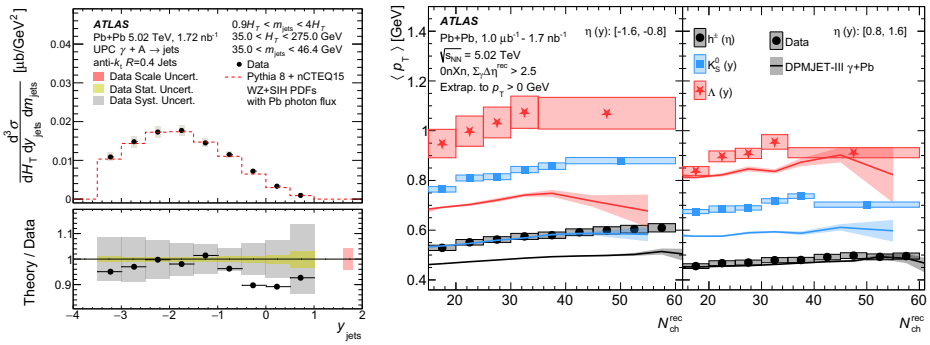

Figure 6. Left: Photonuclear jet cross section vs. y_{jets} for $35 < m_{\text{jets}} < 46.4$ GeV, integrated over H_{T}, compared with PYTHIA (nCTEQ15 WZ+SIH). Right: $\langle p_T \rangle$ of charged hadrons, K_S^0, and Λ vs. N_{ch}^{rec} in Pb+Pb photonuclear collisions for backward/forward rapidity, compared with DPMJET-III (shaded statistical uncertainties) [31].

Photonuclear jet production provides another probe covering a wide Q^2 and x region. Owing to the large jet-production cross-section, a triple-differential measurement was feasible, and the ratio of the results obtained by ATLAS to various nPDF fits was provided [29]. One of the cross-section results of this measurement compared to PYTHIA with nCTEQ15 WZ+SIH PDFs is shown in Fig. 6 This measurement may provide valuable input to nPDF fits.

Finally, photonuclear events with high multiplicities have been observed to exhibit non-zero flow [30], motivating a more detailed ATLAS search for QGP-like signatures [31]. At nucleus-going rapidities, many observables resemble those in p+Pb collisions at similar multiplicities. However, some properties, such as the radial flow shown in Fig. 6, are not well described by current models, preventing strong conclusions about possible QGP formation.

4 Conclusions

The exploration of photon-induced interactions in ultraperipheral heavy-ion collisions continues to provide important insights into both fundamental particle interactions and nuclear structure. Photon-photon interactions have proven to be precise tests of the Standard Model

and helped explore possible Beyond Standard Model phenomena. Additionally, the study of photonuclear interactions has opened new avenues for understanding nuclear gluon densities and fluctuations, through measurements of the vector meson production. The results from recent measurements of jets or D^0-meson production, could be useful to constrain nuclear parton distribution functions.

The results from photonuclear interactions also show interesting challenges, such as discrepancies in measured coherent J/ψ meson production cross-sections and the need for more precise models to describe the observed data. This will aid in understanding of nuclear structure and also in search for the onset of QGP formation in small systems.

As we move forward, the interplay between theoretical predictions and experimental data will remain central to advancing our understanding of nuclear structure and the Standard Model. These findings highlight the importance of ongoing UPC measurements at RHIC and the LHC, also in the context of future Electron-Ion Collider.

References

[1] G. Aad et al. (ATLAS), Phys. Rev. C **104**, 024906 (2021), 2011.12211.
[2] G. Aad et al. (ATLAS), JHEP **2306**, 182 (2023), 2207.12781.
[3] G. Aad et al. (ATLAS), Phys. Rev. Lett. **131**, 151802 (2023), 2204.13478.
[4] A.M. Sirunyan et al. (CMS), Phys. Rev. Lett. **127**, 122001 (2021), 2011.05239.
[5] A. Tumasyan et al. (CMS), Phys. Rev. Lett. **131**, 151803 (2023), 2206.05192.
[6] A. Hayrapetyan et al. (CMS), JHEP **08**, 006 (2025), 2412.15413.
[7] J. Adam et al. (STAR), Phys. Rev. Lett. **127**, 052302 (2021), 1910.12400.
[8] M.I. Abdulhamid et al. (STAR), Phys. Rev. C **110**, 014911 (2024), 2311.13632.
[9] M.I. Abdulhamid et al. (STAR), Phys. Rev. C **111**, 014909 (2025), 2407.14821.
[10] Tech. rep., (ATLAS),CERN, Geneva (2025), note: ATLAS-CONF-2025-004, https://cds.cern.ch/record/2929691
[11] Tech. rep., (CMS), CERN, Geneva (2024), note: CMS-PAS-HIN-24-011, https://cds.cern.ch/record/2912969
[12] G. Aad et al. (ATLAS) (2025), 2504.07795.
[13] G. Aad et al. (ATLAS), Phys. Rev. Lett. **134**, 061803 (2025), 2408.11035.
[14] Tech. rep., (LHCb), CERN, Geneva (2025), note: LHCb-CONF-2024-006, https://cds.cern.ch/record/2929341
[15] V. Chekhovsky et al. (CMS) (2025), 2504.05193.
[16] M.I. Abdulhamid et al. (STAR), Phys. Rev. Lett. **133**, 052301 (2024), 2311.13637.
[17] S. Acharya et al. (ALICE), Phys. Lett. B **798**, 134926 (2019), 1904.06272.
[18] S. Acharya et al. (ALICE), Eur. Phys. J. C **81**, 712 (2021), 2101.04577.
[19] A. Tumasyan et al. (CMS), Phys. Rev. Lett. **131**, 262301 (2023), 2303.16984.
[20] R. Aaij et al. (LHCb), JHEP **07**, 117 (2022), 2107.03223.
[21] Tech. rep., (ATLAS), CERN, Geneva (2025), note: ATLAS-CONF-2025-003, https://cds.cern.ch/record/2929557
[22] S. Acharya et al. (ALICE) (2025), 2503.18708.
[23] V. Chekhovsky et al. (CMS) (2025), 2503.08903.
[24] Tech. rep., (CMS), CERN, Geneva (2025), note: CMS-PAS-HIN-24-013, https://cds.cern.ch/record/2931418
[25] M. Abdallah et al. (STAR), Sci. Adv. **9**, eabq3903 (2023), 2204.01625.
[26] S. Acharya et al. (ALICE), Phys. Rev. Lett. **132**, 162302 (2024), 2305.06169.

[27] Tech. rep., (CMS), CERN, Geneva (2025), note: CMS-PAS-HIN-25-002, https://cds.cern.ch/record/2930669
[28] Tech. rep., (CMS), CERN, Geneva (2024), note: CMS-PAS-HIN-24-003, https://cds.cern.ch/record/2910905
[29] G. Aad et al. (ATLAS), Phys. Rev. D **111**, 052006 (2025), 2409.11060.
[30] G. Aad et al. (ATLAS), Phys. Rev. C **104**, 014903 (2021), 2101.10771.
[31] G. Aad et al. (ATLAS), Phys. Rev. C **111**, 064908 (2025), 2503.08181.